

# Microphotoluminescence and Raman scattering study of defect formation in diamond films

Cite as: Journal of Applied Physics **73**, 3951 (1993); <https://doi.org/10.1063/1.352858>

Submitted: 30 September 1992 • Accepted: 17 December 1992 • Published Online: 04 June 1998

L. Bergman, B. R. Stoner, K. F. Turner, et al.



View Online



Export Citation

## ARTICLES YOU MAY BE INTERESTED IN

[Raman and photoluminescence analysis of stress state and impurity distribution in diamond thin films](#)

Journal of Applied Physics **78**, 6709 (1995); <https://doi.org/10.1063/1.360495>

[The origin of the broadband luminescence and the effect of nitrogen doping on the optical properties of diamond films](#)

Journal of Applied Physics **76**, 3020 (1994); <https://doi.org/10.1063/1.357508>

[Nitrogen induced increase of growth rate in chemical vapor deposition of diamond](#)

Applied Physics Letters **68**, 759 (1996); <https://doi.org/10.1063/1.116733>



Applied Physics  
Reviews

Read. Cite. Publish. Repeat.

**19.162**  
2020 IMPACT FACTOR\*

# Microphotoluminescence and Raman scattering study of defect formation in diamond films

L. Bergman, B. R. Stoner, K. F. Turner, J. T. Glass, and R. J. Nemanich  
*Department of Physics and Department of Materials Science and Engineering,  
North Carolina State University, Raleigh, North Carolina 27695-8202*

(Received 30 September 1992; accepted for publication 17 December 1992)

Photoluminescence and Raman spectroscopy are employed to explore the time evolution of defect formation in chemical vapor deposition diamond films for stages of growth spanning nucleation to continuous film formation. Our research is concentrated on three types of defects which give rise to the 1.68 eV optical band, the  $sp^2$  phase which centers at  $1500\text{ cm}^{-1}$ , and the broadband luminescence at 565–800 nm. The investigation of these types of defects suggests the following conclusions. Si atoms are most likely responsible for the creation of the 1.68 eV optical centers which takes place at the initial stages of growth. Plasma interactions with the Si substrate contribute to the 1.68 eV defect formation. The broad luminescence and  $sp^2$  bonding defects were not present in the isolated nuclei but were significantly present when a continuous film was formed. Two rates of diamond growth were obtained and the changes of the rates were attributed to the lowering degree of freedom available for the growth of the nuclei as well as to the formation of the  $sp^2$  phase.

## I. INTRODUCTION

Investigation of defect formation in chemical vapor deposition (CVD) diamond films is critical in understanding the basic mechanisms of electronic transport and optical interactions which underlie applications in developing electronic and optical devices. In this study Raman and photoluminescence (PL) microscopy was employed to investigate the formation over time of defects in CVD diamond, from the very early stages of diamond nucleation through formation of groups of particles and finally to the growth of continuous thick films. At each stage of the growth, the morphology of the sample was obtained from scanning electron microscope (SEM) images and this information was correlated to the PL and to the Raman line intensities of the defects. This article presents an analysis of the creation of three types of defects associated with optical bands referred to as the 1.68 eV, the  $sp^2$ -type bonding, and the broadband luminescence at 565–800 nm, for stages of growth spanning nucleation to continuous film formation.

One part of our experiment examined the 1.68 eV defect center, for which conflicting models have been proposed. Previous work has suggested a relation of the 1.68 eV center to the GR1 optical active center which exists in natural and synthetic diamond. Upon interaction with light the GR1 gives rise to the photoluminescence band at 1.673 eV. The GR1 defect center can be produced in any type of natural or synthetic diamond by the introduction of radiation damage into the diamond,<sup>1–4</sup> which creates vacancies and interstitials of carbon atoms. It is commonly accepted that the GR1 band is associated with the natural vacancy center which possesses tetrahedral symmetry<sup>5</sup> and has an unpolarized zero-phonon line emission of 1.673 eV arising from a transition between the  $T_2$  and the  $E$  state.<sup>6</sup>

In many thin diamond films grown from the vapor phase, the PL emission line can be observed at 1.68 eV which is a shift of 7 meV from the GR1 peak of the natural

diamond. This shift may indicate that the 1.68 eV center originates from a different defect center than the natural vacancy. Various works show evidence that the introduction of Si during growth increases the 1.68 eV peak significantly.<sup>7,8</sup> One explanation was that the Si atoms were incorporated into the diamond octahedral lattice sites and formed a radiative center there.<sup>7</sup> Another study on Si-implanted natural diamond showed that the 1.68 eV center was due to defects containing two interstitial silicon atoms.<sup>9</sup> Yet another possible explanation for the 7 meV shift is that it arises from the presence of the internal stress which exists in the individual crystallites of the CVD diamond films. This residual stress can induce the 6–7 meV shift of the GR1 center.

Another part of our experiment examined the broadband luminescence. The broad luminescence band, extending from approximately 565 to 800 nm and centered at around 608 nm, has been observed in various luminescence studies. The broadband is exhibited in both cathodoluminescence (CL) spectra of natural and polycrystalline diamond,<sup>10–16</sup> and has also been observed in the PL spectra of other studies.<sup>15–17</sup> In most of the PL and CL spectra, the 2.15 eV center was detected as well. This center has been attributed to the zero-phonon line (ZPL) of the interstitial nitrogen-vacancy complex. It has been suggested that the broad luminescence band is the result of vibronic interaction corresponding to the 2.15 eV ZPL.<sup>13</sup> Inspection of the PL spectra of hydrogenated amorphous carbon<sup>18,19</sup> reveals that a broadband luminescence exists with similar characteristics as the diamond broadband PL/CL. However, since the CVD diamond film was found to possess  $sp^2$  amorphous-like carbon bonding, it is surmised that the broadband luminescence may be due to that type of defect.

In this article the experimental results and analysis of the formation of 1.68 eV,  $sp^2$ -type and broadband luminescence defects is presented. Section III A of this article describes measurements of the Raman linewidth, the ratio of

the  $sp^2$ -type bonding to the  $sp^3$  diamond-type bonding ( $sp^2/sp^3$ ), and the absolute integrated diamond Raman line intensities as a function of the growth time. At the very early stages of the deposition when the morphology of the substrate consisted of isolated diamond particles, no  $sp^2$  phase was found and the Raman linewidth exhibited a decrease with time. Furthermore the integrated diamond line followed a power-law increase with time. At later stages when coalescing of particles took place,  $sp^2$ -type bonding was found to form linearly with deposition time and the diamond linewidth increased monotonically with time. Also, the integrated diamond line still exhibited a power-law increase but with a smaller exponent than at earlier stages of growth. From the analysis of Raman linewidth and diamond intensity, a common critical threshold time was obtained which separated the early growth time phenomena from the longer time events, corresponding to the time when the diamond particles just started to coalesce as observed in the SEM images.

Section III B reports a study of the 1.68 eV defect center. The PL measurements indicated that the formation of the 1.68 eV centers takes place at very early stages of nucleation and growth of the diamond particles. The rate of incorporation of the defects into the growing film diminishes as the sample becomes continuous. It is hypothesized that plasma etching of the Si substrate is a possible mechanism to provide Si atoms which enhance the formation of the 1.68 eV optical centers. This hypothesis about the interaction of plasma and Si substrate was checked via an experiment in which five diamond films were grown at different distances from the plasma. The 1.68 eV relative intensities of these samples were significantly higher for the samples which were placed next to the plasma core than for the samples which were located farther away.

In Sec. III C preliminary results of the study on the broadband luminescence are presented. The initial analysis indicates that the type of defects responsible for the broad PL does not exist in the isolated diamond nuclei, but rather tend to be created in later stages of growth. The broad PL follows similar growth versus time behavior as the  $sp^2$  phase, and therefore it is suggested that the amorphous  $sp^2$ -bonded carbon contributes to the broad PL in the CVD diamond film.

## II. EXPERIMENT

Diamond samples for this study were grown in an AS-TeX stainless steel microwave plasma CVD chamber described in detail in previous publications.<sup>20,21</sup> Briefly, the chamber consists of a cylindrical stainless steel cavity with an inner diameter of 6 in. The plasma forms in a stable position at the center of the cavity and the substrate may be positioned relative to the plasma up to 8 cm downstream. The Si (100) substrates in this study were prepared by first abrading them with 1  $\mu\text{m}$  diamond paste in order to increase the nucleation density of the diamond particles. The abrasion was followed by an ultrasonic cleaning in TCE, acetone, and methanol, a rinse with de-ionized (DI) water, and then dried with nitrogen.

For the study of defect formation as a function of time, a series of stop-growths was performed. The growth sequence was interrupted after deposition times of 1.5, 3, 5, 7, 10, 17, and 40 h. Each step of the growth was followed by SEM, Raman microscopy, and photoluminescence analysis. Following the analysis, the sample was solvent-cleaned as discussed above and then reinserted into the growth chamber. The sample was grown in an immersed mode and was located 0.5 cm into the plasma. The plasma consisted of 1%  $\text{CH}_4$  in  $\text{H}_2$  at 1000 sccm total flow. The plasma power, chamber pressure, and substrate temperature were maintained at 800 W, 25 Torr, and 750  $^\circ\text{C}$ , respectively. For the study of the role of plasma in defect creation, five diamond samples were grown on Si substrates at positions 0, 1, 2, 3, and 4 cm below the plasma edge.

The photoluminescence and microwave Raman spectroscopy were carried out at room temperature using the ISA U-1000 scanning monochromator. The samples were excited with the 514.5 nm line of an Argon-ion laser, which was focused on the sample to a spot of about 5  $\mu\text{m}$  diameter. Focusing was facilitated by using the Olympus BH-2 microscope. The laser power at the sample was measured to be about 20 mW. The Raman spectra were taken at the region 1000–1800  $\text{cm}^{-1}$  and the PL spectra were taken at the region 400–7000  $\text{cm}^{-1}$  (2.36–1.54 eV). In order to check the spatial variation and to improve statistical significance the Raman and the PL data were taken at 12 different locations on the sample for each stage of the experiment. The data reported in this article represent an average of these 12 points.

## III. RESULTS AND DISCUSSION

### A. Analysis of the diamond and the graphitic Raman spectra

The first part of our experiment focused on an analysis of the Raman spectra as a function of growth time. In the Raman spectra of our cyclic growth sample, two main Raman features centered at 1332 and at 1500  $\text{cm}^{-1}$  were observed. The Raman scattering at 1332  $\text{cm}^{-1}$  has proved to be an indication of  $sp^3$  diamond bonding while the broad feature at 1500  $\text{cm}^{-1}$  has been attributed to  $sp^2$  amorphous-type graphitic bonding.<sup>22–26</sup>

The diamond Raman linewidth, full width at half maximum (FWHM), was first analyzed as a function of deposition time. Figure 1 shows the FWHM plotted as a function of growth time. The linewidth exhibits a minimum at about 8 h and a monotonic increase thereafter. The relatively large linewidth at 1.5 h and 3 h of growth time may be attributed to the grain-size broadening mechanism of the small nuclei<sup>27</sup> as well as to the incorporation of the relatively large Si atoms into the diamond matrix which takes place at early stages as will be discussed in Sec. III B of this article. The minimum Raman linewidth occurs at around 8 h when the diamond particles are large (about 1.5  $\mu\text{m}$ ), and for the most part are isolated and just beginning to cluster as indicated by the SEM images shown in Fig. 2. The broadening of the linewidth at the later stages of deposition when the particles coalesce and a continuous

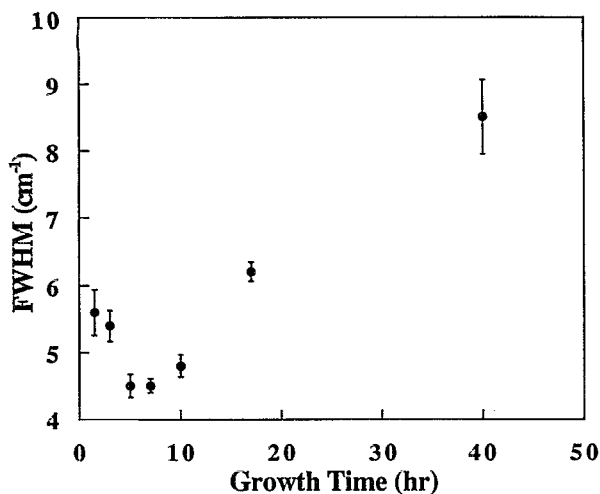


FIG. 1. The diamond Raman linewidth (FWHM) as a function of deposition time. The optimum of the linewidth occurs at  $\sim 8$  h.

film forms can be attributed to three possible broadening mechanisms: the inhomogeneous strain induced by the increasing concentration of the grain boundaries in the film, the increasing presence of the  $sp^2$ -type defects, and the size effect of the secondary nucleation.

Next the diamond Raman integrated intensity as well as the  $sp^2/sp^3$  ratio was analyzed as a function of deposition time. Figure 3 shows the Raman spectra at the seven stages of growth time. The  $sp^2$  feature at  $1500\text{ cm}^{-1}$  starts to be noticeable at around 7 to 10 h of growth time and becomes relatively large thereafter. For growth times under 7 h the  $sp^2$  feature was hard to detect in the spectra. Figure 4 shows for the same Raman spectra the plot of  $sp^2/sp^3$  ratio

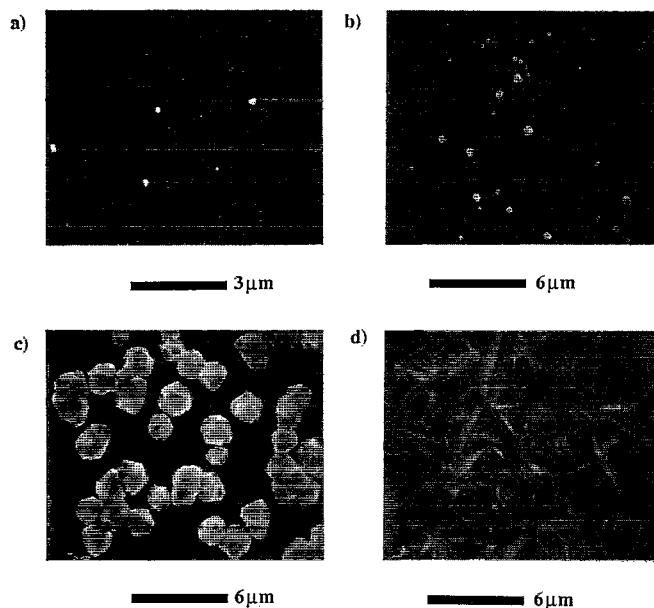


FIG. 2. The SEM micrographs of the diamond sample at (a) 1.5, (b) 3, (c) 10, and (d) 40 h of deposition time.

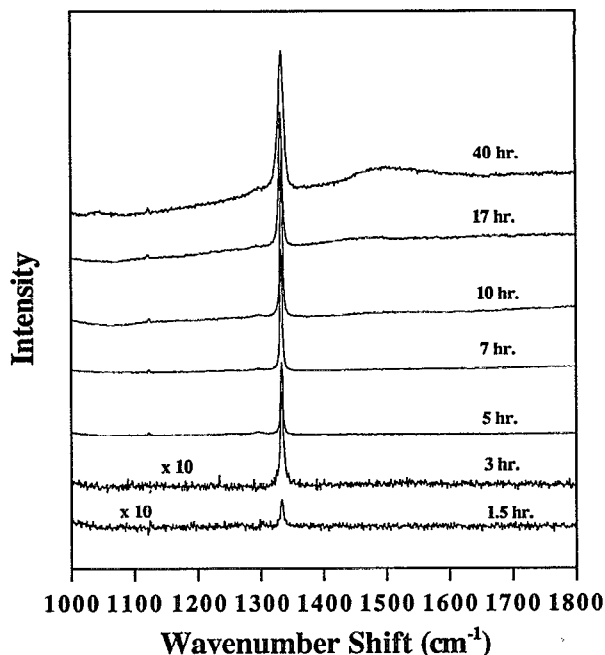


FIG. 3. The Raman spectra at the seven stages of deposition time: 1.5, 3, 5, 7, 10, 17, and 40 h.

versus growth time. The plot indicates the absence of  $sp^2$  defects until around 7 h and a linear increase for longer growth times.

The growth rate of CVD diamond is controlled by a complex dynamic balancing of the competitive growth of  $sp^2$  and  $sp^3$  phases and the preferential etching of  $sp^2$  by atomic hydrogen.<sup>28,29</sup> Determination of the growth mechanism and the kinetics of the CVD diamond is beyond the scope of this research, but the following data suggests several tentative conclusions.

The absence of  $sp^2$ -type defects at 1.5, 3, 5, and 7 h of growth time, at which stages the morphology was observed to be one of unconnected nuclei of random orientation, may be the result of the preferential etching of the defects by the atomic hydrogen. Kobashi *et al.*<sup>29</sup> have found that

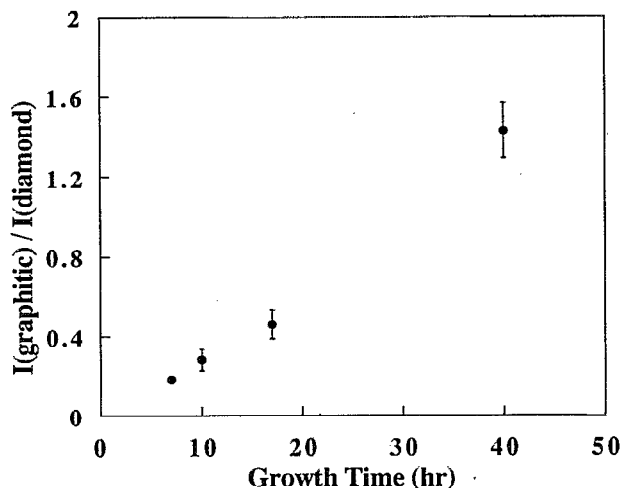


FIG. 4. The relative Raman intensity of the  $sp^2$ -type bonding vs growth time. The graphitic component is not present in the spectra at the early stages of growth (1.5–7 h).

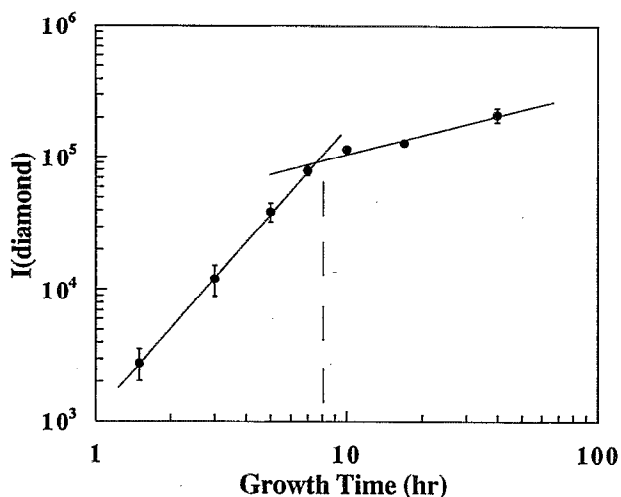


FIG. 5. The integrated intensity of the diamond Raman peak as a function of growth time. The transition from higher to lower growth rate occurs at  $\sim 8$  h.

the chemical reaction rate of graphite with hydrogen is about 30 times faster than that of diamond. Therefore,  $sp^2$ -type clusters are removed rapidly from the substrate surface and only diamond grains remain and grow. If this is the main mechanism preventing the presence of  $sp^2$ -type defects at early stages, then the rate of growth of  $sp^2$ -type defects should be approximately equal to the rate of its removal.

At later stages when coalescing and clustering of the nuclei occur resulting in the formation of grain boundaries, the  $sp^2$  phase follows a linear increase with deposition time. This implies that the rate of growth of  $sp^2$ -type defects is higher than the rate of its etching by the atomic hydrogen. One possible mechanism for the change in rate which takes place at around 8 h is incipient formation at that time of grain boundaries where particles join. The grain boundaries may provide favorable sites for the  $sp^2$  phase to nucleate and grow. The hypothesis that  $sp^2$ -type bonding is present predominantly at grain boundaries was also stated in the work of other groups.<sup>30,31</sup>

In order to determine how the diamond growth rate is impacted by the initial incorporation of the  $sp^2$ -type defect and the morphology transition from isolated nuclei to clusters, the integrated intensity of the diamond Raman peak versus time was calculated. Figure 5 shows the plot of the diamond integrated intensity as a function of growth time. The plot indicates two different power-law growth rates of the diamond, and a transition time at around 8 h. This transition time is consistent with the time of the initial appearance of the  $sp^2$  defect and the time when a change in the morphology takes place.

The growth rate is higher at early stages when nuclei are isolated from one another and space is available for the grains to grow in both lateral and vertical directions. Above the transition time the growth rate is lowered due to the coalescing which reduces the lateral degree of freedom available for the growth of the nuclei, as well as due to the

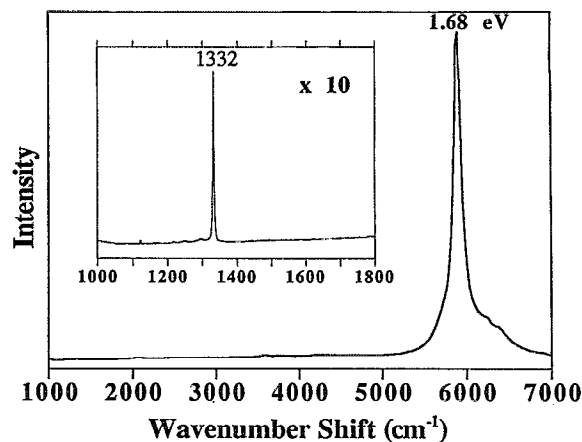


FIG. 6. The PL and Raman spectra of the diamond particles at 7 h of growth time.

competitive formation of the  $sp^2$  phase in the growing film as discussed in the previous paragraphs.

### B. The 1.68 eV optical center

In the second part of this study the formation of the 1.68 eV centers as a function of growth time was examined. Figure 6 shows the spectra of the 1.68 eV band at 7 h of growth time. For the cyclic growth sample, the PL integrated intensity of the 1.68 eV line was calculated and normalized to the diamond integrated Raman line for various growth times. The results shown in Fig. 7 indicate an initial increase of the 1.68 eV relative intensity until a maximum is reached at about 8 h; thereafter the PL relative line is seen to decrease with increasing growth time. The SEM images of this sample shown in Fig. 2 reveal that initially the film consists of isolated diamond particles; after  $\sim 8$  h the diamond particles start to coalesce, forming grain boundaries until most of the Si substrate is covered by the growth.

A possible mechanism for the effect shown in Fig. 7 is that etching of the Si substrate by the plasma releases Si atoms in the gas phase and allows them to become incorporated into the growing diamond film. In the early stages when the nucleation and growth of the isolated particles

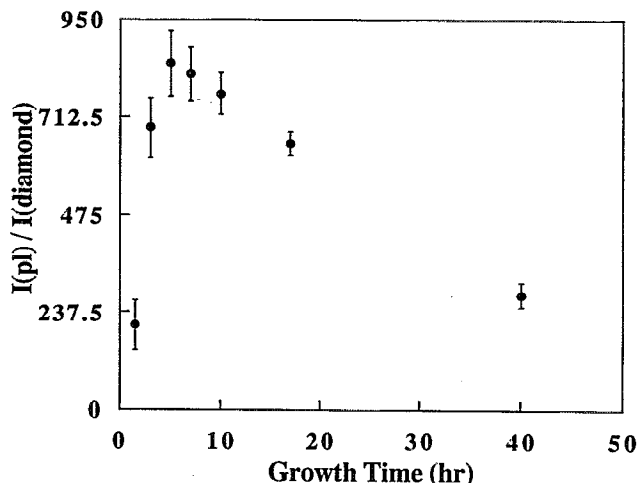


FIG. 7. The relative integrated PL intensity of the 1.68 eV band as a function of deposition time. The highest intensity occurs at  $\sim 7$  h.

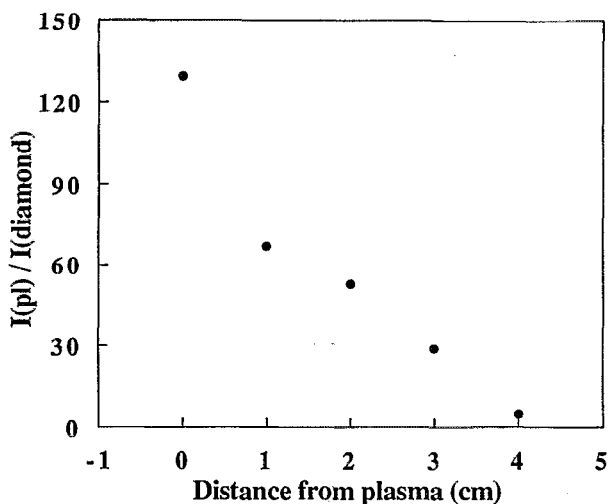


FIG. 8. The relative integrated PL intensity of the 1.68 eV band vs distance from the plasma during growth.

take place, the probability of creating the 1.68 eV centers is high since the Si substrate is almost entirely exposed to the plasma. As the diamond nuclei continue to grow in an isolated fashion, the concentration of the defect centers increases. At deposition times longer than 8 to 10 h, less of the Si substrate is exposed to the plasma, resulting in a reduced concentration of the 1.68 eV defect centers.

The absolute integrated intensity of the 1.68 eV line was also measured at ten different positions on the 10 h growth sample. No significant variation in intensity was found which implies that the final spatial distribution of these defects was nearly uniform across the sample. For the sample of 40 h growth time, large fluctuations in the 1.68 eV absolute intensities were observed across the sample. Furthermore, on average, the PL intensity was 35% lower than the absolute integrated intensity exhibited by the 10 h sample which possessed the maximum concentration of defects. The diamond Raman signal also exhibited up to 30% variation in intensity across the sample. The above observations suggest that the film thickness and the presence of grain boundaries caused the luminescence of the 40 h sample to scatter, thereby making the PL signal hard to collect. This scattering of the luminescence implies that the 1.68 eV defect centers reside mainly next to the interface of the diamond and the Si substrate.

To support the assumption that plasma interaction with Si substrate initiates formation of the optical defect centers, five incomplete diamond films were grown at different distances from the hydrogen plasma. Figure 8 shows the resulting 1.68 eV integrated relative intensity as a function of distance from the plasma, and indicates that the film which was grown nearest the plasma (i.e., immersed in it) exhibited the highest concentration of the 1.68 eV centers. The film which was grown 4 cm from the plasma exhibited very small concentrations of these centers. Saito *et al.*<sup>32</sup> have found other evidence of hydrogen plasma interaction with the Si substrate: their experiments revealed that when placing the Si substrate in the plasma center,

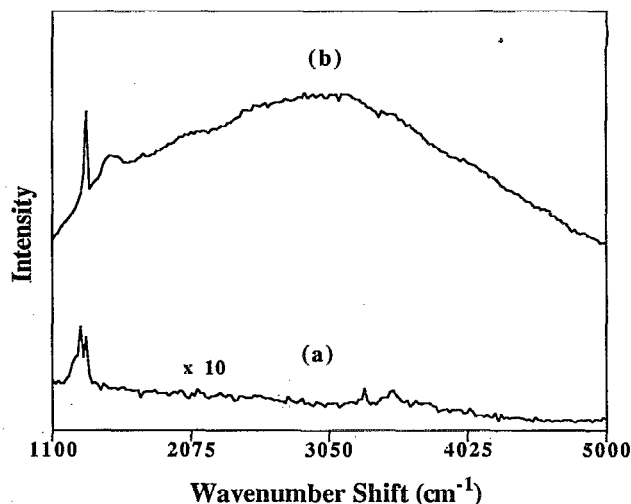


FIG. 9. The broad PL spectra of (a) the isolated nuclei at 3 h and (b) of the continuous film at 40 h of growth time.

etching and redeposition of Si atoms was the predominant reaction due to the high concentration of electrons and hydrogen radicals.

### C. The broadband PL at 565–800 nm

An analysis of the broadband photoluminescence as a function of growth time is now presented. Figure 9 shows the broadband PL spectra for the isolated diamond nuclei at 3 h of growth time and for the continuous film at 40 h. The spectra of the continuous film exhibits a strong PL band ranging from approximately 1000 to 6000  $\text{cm}^{-1}$  (565–800 nm), and centered at around 2 eV ( $\sim 3000 \text{ cm}^{-1}$ ). The broadband PL is not present in the spectra of the isolated diamond nuclei.

The graph of the relative integrated intensity of the PL band versus growth time is shown in Fig. 10. The PL band was not observed in the spectra of the initial stages of growth, and was noticeable only from 7 to 40 h during

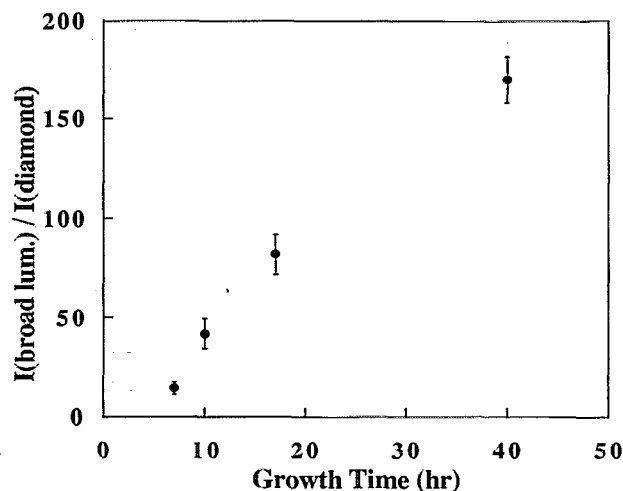


FIG. 10. The relative integrated intensity of the broadband PL vs deposition time. The broadband is not present in the spectra at the early stages of growth.

which interval it behaved linearly with growth time. The time evolution of the broadband PL is similar to that of the  $sp^2$ -type bonding (see Fig. 4). The similarity in the formation of the two types of defects may be an indication that the presence of defects which caused the broad PL is due to the  $sp^2$  carbon bonding which exists in disordered configuration in the diamond film.

Broadband PL spectra very similar to those found in our work have been observed in many studies of amorphous hydrogenated carbon material ( $a$ -C:H) which possess a random network of  $sp^2$  and  $sp^3$  bonding configuration.<sup>18,19</sup> The lineshape and the peak position of the PL was found in these studies to vary from sample to sample depending on the growth condition. The broad PL in  $a$ -C:H has been assumed to originate from transitions in the exponential distribution of tail states which extend into the forbidden gap. The presence of tail states is a consequence of the lost long-range order in the material.

Other studies using cathodoluminescence (CL) spectroscopy suggest that the broad luminescence in diamond is due to interaction of the 2.16 eV ZPL center with the lattice vibration (vibronic interaction).<sup>10,12-14</sup> The 2.16 eV band which arises from the interstitial nitrogen-vacancy complex was observed in our spectra and had a very weak intensity. The nitrogen in the diamond film was probably deposited from the residual amount of this element which existed in the environment of the growth chamber.

The fact that both PL and CL extend over the same range of luminescence and have similar lineshape does not exclude the possibility that CL is due to a different type of defect center than that of PL, since the two spectroscopies differ in their energy range and in their cross section. The determination of the origin of the broad luminescence will be addressed in a future study.

From the present data it can be concluded that the type of defect responsible for the broadband PL in the CVD diamond does not form at early stages when isolated nuclei constitute the morphology. The defects instead start to form at approximately 7 h of growth time and have increasing concentration thereafter. A possible type of defect which may cause this broad PL is the amorphous  $sp^2$ -type bonding which has time evolution consistent with the PL luminescence intensity.

#### IV. CONCLUSIONS

The following conclusions about the formation of defects in CVD diamond films are suggested by the study:

(1) The diamond linewidth exhibits an optimum when the particles are large and disconnected. As the film became continuous, a broadening of the line was observed, and was attributed to the strain induced by the grain boundary and to the  $sp^2$  phase, both of which appear at later stages of the growth.

(2) The Raman spectra revealed that the isolated nuclei did not contain  $sp^2$ -type defects. At later stages when clustering occurred and grain boundaries formed, the  $sp^2$  phase was found to increase with growth time. The increase of the  $sp^2$  defect concentration may be attributed to

the presence of the grain boundaries which provide sites for the  $sp^2$ -type bonding.

(3) From any analysis of the integrated diamond Raman lines as a function of time, a characteristic time was obtained for which a morphological transition of isolated nuclei to clusters took place. The characteristic time marked also the time when the  $sp^2$  phase started to appear. It is surmised that these two events were responsible for the decreased growth rate of the diamond.

(4) The 1.68 eV defects are found to be created mostly at early stages of diamond nucleation and growth when most of the substrate is exposed to the plasma. Hence higher concentrations of this type of defect reside in the vicinity of the Si substrate and less in the bulk of the diamond film. In our experiment, no variation in concentration of the 1.68 eV defect was found across the sample.

(5) The plasma interaction with the Si substrate is essential to the formation of the 1.68 eV defect in the CVD diamond. Since the creation of the optical center is greatly enhanced by the availability of Si, most likely the center contains Si atoms. This conclusion is supported by our observations that the relative integrated intensity of the 1.68 eV band of the samples, which were grown in various distances from the plasma, exhibited a decrease with distance from the plasma, combined with the finding that the creation of the defects took place at early stages when most of the Si substrate was exposed to the plasma.

(6) The broad PL band which centers at  $\sim 2$  eV was not observed in the spectra of the early stages of nucleation and growth, but was present in the spectra of the later stages. The broad PL and the  $sp^2$  intensities both follow similar time evolution. Amorphous carbon hydrogenated material, which contains the same bond configuration as the  $sp^2$  phase in the diamond film,<sup>18,19</sup> exhibits broad photoluminescence spectra similar to that observed in our spectra. These two observations lead us to suggest that the  $sp^2$  bonding configuration may give rise to the broadband luminescence. This topic will be investigated in a future study.

In summary, the isolated diamond nuclei contain only the 1.68 eV optical defect. The diamond bulk film contains the  $sp^2$ -type defects and the defects which give rise to the broad PL.

#### ACKNOWLEDGMENTS

We gratefully acknowledge the support of the Office of naval Research through grants N00014-90-J-1604 and N00014-92-J-1477.

<sup>1</sup>C. D. Clark and J. Walker, Proc. Roy. Soc. London A 234 (1973).

<sup>2</sup>C. D. Clark and E. W. J. Mitchell, in *Proceedings of the 1970 Conference on Radiation Damage in Semiconductors*, edited by J. W. Corbett and G. D. Watkins (Gordon and Breach, London, 1971), p. 257.

<sup>3</sup>A. M. Stoneham, *Theory of Defects in Solids* (Clarendon, Oxford, 1975).

<sup>4</sup>J. Walker, Rep. Prog. Phys. **42**, 1605 (1979).

<sup>5</sup>G. Davis, in *Chemistry and Physics of Carbon* **13**, 2 (1977).

<sup>6</sup>C. D. Clark and C. A. Norris, J. Physics C: Solid State Phys. **4**, 2223 (1971).

<sup>7</sup>A. R. Badzian, T. Badzian, R. Roy, R. Messier, and K. E. Spear, Mater. Res. Bull. **23**, 531 (1988).

- <sup>8</sup>J. Ruan, W. J. Choyke, and W. D. Partlow, *Appl. Phys. Lett.* **58**, 295 (1991).
- <sup>9</sup>V. S. Vavilov, A. A. Gippius, A. M. Zaitsev, B. V. Deryagin, B. V. Spitsyn, and A. E. Aleksenko, *Sov. Phys. Semicond.* **14**, 1078 (1980).
- <sup>10</sup>G. Davies, *J. Phys. C: Solid State Phys.* **12**, 2551 (1979).
- <sup>11</sup>R. J. Graham and K. V. Ravi, *Appl. Phys. Lett.* **60**, 1310 (1992).
- <sup>12</sup>A. T. Collins and S. H. Robertson, *J. Mater. Sci. Lett.* **4**, 681 (1985).
- <sup>13</sup>L. H. Robins, L. P. Cook, E. N. Farabaugh, and A. Feldman, *Phys. Rev. B* **39**, 39 (1989).
- <sup>14</sup>A. M. Zitsev, A. A. Gippius, and V. S. Vavilov, *Sov. Phys. Semicond.* **16**, 252 (1982).
- <sup>15</sup>E. S. Etz, E. N. Farabaugh, A. Feldman, and L. H. Robins, *SPIE* **969**, 86 (1988).
- <sup>16</sup>J. A. Freitas, Jr., J. E. Butler, and U. Strom, *J. Mater. Res.* **5**, 2502 (1990).
- <sup>17</sup>D. S. Knight and W. B. White, *SPIE* **1055**, 144 (1989).
- <sup>18</sup>S. Lin and B. J. Feldman, *Phys. Rev. Lett.* **48**, 829 (1982).
- <sup>19</sup>J. Wagner and P. Lautenschlager, *J. Appl. Phys.* **59**, 2044 (1986).
- <sup>20</sup>B. R. Stoner, J. T. Glass, L. Bergman, R. J. Nemanich, L. D. Zoltan, and J. W. Vandersande, *J. Electron. Mater.* **21**, 629 (1992).
- <sup>21</sup>B. R. Stoner, G.-H. M. Ma, S. D. Wolter, and J. T. Glass, *Phys. Rev. B* **45**, 11067 (1992).
- <sup>22</sup>R. J. Nemanich, J. T. Glass, G. Lucovsky, and R. E. Shroder, *J. Vac. Sci. Technol. A* **6**, 1783 (1988).
- <sup>23</sup>R. J. Nemanich and S. J. Solin, *Phys. Rev. B* **20**, 392 (1979).
- <sup>24</sup>L. H. Robins, E. N. Farabaugh, and A. Feldman, *J. Mater. Res.* **5**, 2456 (1990).
- <sup>25</sup>L. H. Robins, E. N. Farabaugh, and A. Feldman, *SPIE* **1325**, 131 (1990).
- <sup>26</sup>D. S. Knight and W. B. White, *J. Mater. Res.* **4**, 385 (1989).
- <sup>27</sup>Y. M. LeGrice, R. J. Nemanich, J. T. Glass, Y. H. Lee, R. A. Rudder, and R. J. Markumas, *Mater. Res. Soc. Symp. Proc.* **162**, 219 (1990).
- <sup>28</sup>A. R. Badzian and R. C. DeVries, *Mater. Res. Bull.* **23**, 385 (1988).
- <sup>29</sup>K. Kobashi, K. Nishimura, Y. Kawate, and T. Horiuchi, *Phys. Rev. B* **38**, 4067 (1988).
- <sup>30</sup>Y. Sato and M. Kamo, *Surf. Coatings Technol.* **39/40**, 183 (1989).
- <sup>31</sup>A. V. Hetherington, C. J. H. Wort, and P. Southworth, *J. Mater. Res.* **5**, 1591 (1990).
- <sup>32</sup>Y. Saito, S. Matsuda, and S. Nogita, *J. Mater. Sci. Lett.* **5**, 565 (1986).